

Soil identification and chemometrics for direct determination of nitrate in soils using FTIR-ATR mid-infrared spectroscopy

Raphael Linker ^{*}, Itzhak Shmulevich, Amit Kenny, Avi Shaviv

*Faculty of Civil and Environmental Engineering, Lowdermilk Division of Agricultural Engineering,
Technion-Israel Institute of Technology, Haifa 32000, Israel*

Received 28 September 2004; received in revised form 7 March 2005; accepted 11 March 2005
Available online 26 April 2005

Abstract

The use of mid-infrared attenuated total reflectance (ATR) spectroscopy enables direct measurement of nitrate concentration in soil pastes, but strong interfering absorbance bands due to water and soil constituents limit the accuracy of straightforward determination. Accurate subtraction of the water spectrum improves the correlation between nitrate concentration and its ν_3 vibration band around 1350 cm^{-1} . However, this correlation is soil-dependent, due mostly to varying contents of carbonate, whose absorbance band overlaps the nitrate band. In the present work, a two-stage method is developed: First, the soil type is identified by comparing the “fingerprint” region of the spectrum ($800\text{--}1200\text{ cm}^{-1}$) to a reference spectral library. In the second stage, nitrate concentration is estimated using the spectrum interval that includes the nitrate band, together with the soil type previously identified. Three methods are compared for estimating nitrate concentration: integration of the nitrate absorbance band, cross-correlation with a reference spectrum, and principal component analysis (PCA) followed by a neural network. When using simple band integration, the use of soil specific calibration curves leads to determination errors ranging from 5.5 to 24 mg[N]/kg[dry soil] for the mineral soils tested. The cross-correlation technique leads to similar results. The combination of soil identification with PCA and neural network modeling improves the predictions, especially for soils containing calcium carbonate. Typical prediction errors for light non-calcareous soils are about 4 mg[N]/kg[dry soil], whereas for soils containing calcium carbonate they range from 6 to 20 mg[N]/kg[dry soil], which is less than four percent of the concentration range investigated.

© 2005 Elsevier Ltd. All rights reserved.

Keywords: Cross-correlation; Neural network; Principal component analysis (PCA); Soil constituents interference

1. Introduction

Direct and fast monitoring of nitrate in soils is extremely important for managing fertilizer application and controlling nitrate leaching. Such monitoring would allow adjusting fertilization levels to ‘local’ field requirements (precision farming), thus reducing both

^{*} Corresponding author. Tel.: +972 4 829 5902; fax: +972 4 829 5696.

E-mail address: linkerr@tx.technion.ac.il (R. Linker).

fertilization costs and nitrate pollution. However, due to technological limitations, in situ or near real-time monitoring of soil nitrate is currently not feasible. The most promising methods under investigation and/or development appear to be nitrate selective electrodes (e.g. Adsett et al., 1999), ion sensitive field effect transistor (e.g. Birrell and Hummel, 2000), and mid-infrared spectroscopy (e.g. Ehsani et al., 2001; Shaviv et al., 2003), which is further investigated here.

Mid-infrared spectroscopy, and more particularly attenuated total reflectance (ATR) with Fourier transform infrared-red (FTIR) spectrometers, has been used for the study of liquids, pastes and powders, in which intense scattering of absorption and/or interference of water precludes the use of transmission spectroscopy (e.g. Johnston and Aochi, 1996). Until recently, FTIR/ATR spectroscopy was not used for direct measurement of low concentrations of pollutants in soil pastes or slurries, but rather to investigate chemical processes in the soil (e.g., Elzinga et al., 2001). Shaviv et al. (2003) and Linker et al. (2004) have demonstrated the potential usefulness of the FTIR/ATR technique for direct determination of nitrate concentration in solutions and soil pastes, using the bending vibration band (ν_3) of nitrate located around 1350 cm^{-1} . While standard FTIR/ATR relies on crystals prisms or slabs on which the sample is placed (e.g. Stuart, 1997), Shaviv et al. (2003) also investigated the use of new optic fibers with high transmittance in the mid-IR range (fiberoptic evanescent wave spectroscopy—FEWS, Messica et al. (1996)), which would enable both continuous and remote monitoring. However, as indicated by the results of Shaviv et al. (2003), further improvements of the FTIR/ATR approach are required in order to reduce measurement noise and interference of soil constituents with nitrate. Linker et al. (2004) investigated the use of chemometric methods (principal components regression, partial least squares, and cross-correlation) to overcome interferences, due mostly to the large carbonate band, around

1450 cm^{-1} . The lowest error of estimate in this work, ca $8\text{ mg[N]/kg[dry soil]}$, was obtained for pastes of non-calcareous light soils.

This paper examines an alternative approach, which relies primarily on the assumption that nitrate calibration curves for known soil types can be successfully used to determine nitrate in saturated pastes of “unknown” soil samples, provided the soil sample is correctly identified using a database of spectra (library). Accordingly, the main goals of this work were: (i) to validate the assumption that the soil type of a sample with unknown nitrate concentration can be identified by comparing the sample spectrum with a spectral library of known soils, and (ii) to investigate several chemometric techniques for nitrate determination following soil identification.

2. Materials and method

2.1. Soil preparation and spectral measurements

Table 1 summarizes the characteristics of the seven mineral soils and the peat (Tourbe) used for this work. Soil saturated pastes (moisture content in Table 1) were obtained by adding KNO_3 solutions of predetermined concentrations to the soil samples. For the H2 soil, the added nitrate concentrations ranged from 0 to $870\text{ mg[N]/kg[water]}$ at $30\text{ mg[N]/kg[water]}$ increments, resulting in 30 concentration points. For all the other soils and the peat, the added nitrate concentration ranged from 0 to $1000\text{ mg[N]/kg[water]}$, at $100\text{ mg[N]/kg[water]}$ increments, resulting in 11 concentration points for each soil. Since the soils differed in saturation moisture content, the final concentration on dry soil basis changed accordingly. The ranges of nitrate concentration, on dry soil basis, used for each soil are given in Table 1, and it should be noted that the range for the peat is one order of magnitude larger due to its considerably higher moisture holding capacity.

Table 1
Characteristics of the soils used

Type/classification	Origin or denomination in text	CaCO_3 content (g[CaCO_3]/g[dry soil])	pH	Clay content (g[clay]/g[dry soil])	Organic matter (mg[OM]/g[dry soil])	Moisture content of soil paste (g[water]/g[soil])	Nitrate range tested ^a (mg[N]/kg [dry soil])
Rhodoxeralf	H1	0.00	7.1	0.01	3	0.39	0–490
Rhodoxeralf	H2	0.00	7.1	0.01	~1	0.50	0–435
Ultisol	Ulti	0.00	6.1	0.24	8	0.45	61–440
Histosol	Tourbe	0.00	3.6	<0.01	~900	3.56	0–3390
Inseptisol Typic Umbrandet	Insep	0.01	5.5	0.50	75	0.60	30–550
Enthic Chromoxerert	Shaalabim	0.09	8.0	0.54	16	0.77	17–724
Torrifluent	Bsor	0.13	8.2	0.15	2	0.40	5–387
Torrifluent	Beit Shean	0.47	8.1	0.55	10	0.47	54–468

^a The first value corresponds to initial nitrate-N contained in the soil.

Spectral measurements were performed using a FTIR/ATR spectrometer (Bruker Vector 22) equipped with a ZnSe horizontal crystal and a DGTS detector. The moisture content of the paste was such that it could be easily spread over the whole ATR crystal ($\approx 8 \text{ cm} \times 1 \text{ cm}$). For each sample, the average of 32 successive scans, over the range of $800\text{--}4000 \text{ cm}^{-1}$ with a resolution of 2 cm^{-1} , was recorded. This range covered the two main nitrate bands, namely ν_3 , around 1350 cm^{-1} and the weaker ν_1 around 1040 cm^{-1} ; the soil “fingerprint” around $800\text{--}1200 \text{ cm}^{-1}$; and the two large water bands ν_2 and ν_L centered around 1640 and 750 cm^{-1} , respectively. In addition to the 107 soil spectra, the spectra of de-ionized water and de-ionized water with $1000 \text{ mg[N]/kg[water]}$ were also recorded. Seventy five percent of the spectra were randomly chosen to form the calibration set, the remaining 25% forming the validation set.

2.2. Data processing

2.2.1. Water subtraction and spectra correction

FTIR spectra recorded in similar conditions are generally slightly scaled, biased or tilted relative to each other (e.g. Powell et al., 1986), and these “flaws” must be properly corrected before further analysis. This is important in the present case since the ν_3 nitrate band (around 1350 cm^{-1}) is leaning on the much larger water band (ν_2) centered around 1640 cm^{-1} . In addition, the ν_L water band centered around 750 cm^{-1} is likely to interfere with the soil “fingerprint” region around $800\text{--}1200 \text{ cm}^{-1}$. Simple mathematical subtraction of an average water spectrum is not satisfactory since the bands of the analyte are significantly smaller than the water ones. Several techniques for automatic and accurate subtraction of the water spectrum have been described in the literature (e.g. Powell et al., 1986; Dousseau et al., 1989; Rahmelow and Hübner, 1997). Linker et al. (2004) have adapted such a procedure for nitrate determination, which can be summarized as follows:

1. Choose an interval in which the measured spectrum is due to water only (not affected by nitrate and/or soil). In the present work, the $1550\text{--}2500 \text{ cm}^{-1}$ interval has been chosen.
2. For each spectrum, determine the scaling coefficient such that, in the interval chosen, the difference between the measured spectrum and the scaled water spectrum is as close as possible to a straight line. This straight line is the residual baseline.
3. After subtracting the scaled water spectrum from the measured spectrum, remove the residual baseline.

2.2.2. Soil identification and nitrate determination

Previous studies (e.g. Shaviv et al., 2003; Linker et al., 2004) have shown that a strong correlation

exists between the ν_3 nitrate absorbance band and the nitrate concentration. However, this correlation is soil dependent, and a straightforward approach, such as using the area under the nitrate band as a predictor, regardless of the soil type, leads to very poor results (not shown). Re-examination of the water-subtracted spectra revealed distinct differences between the “fingerprint region” (around $800\text{--}1200 \text{ cm}^{-1}$) of the different soils, indicating that the soil type could be identified using this range. Therefore, a two-stage procedure was devised:

1. Identification of the type of soil, using the information contained in the $800\text{--}1200 \text{ cm}^{-1}$ “fingerprint region”.
2. Determination of the nitrate concentration, using the region of the ν_3 nitrate absorbance band and the specific calibration curve of the soil identified.

2.2.2.1. Soil identification. After creating a library composed of the spectra of the soil pastes with no added nitrate, the coefficient of correlation between the $800\text{--}1200 \text{ cm}^{-1}$ interval of an “unknown” spectrum and the corresponding interval in the spectra contained in the library was calculated. The coefficient of correlation between the spectra S_1 and S_2 is defined as

$$\Gamma(S_1, S_2) = C(S_1, S_2) / \sqrt{C(S_1, S_1)C(S_2, S_2)} \quad (1)$$

where $C(S_1, S_2)$ is the covariance of the matrix containing the spectra S_1 and S_2 . The unknown spectrum was identified as the soil with which it had the highest coefficient of correlation.

2.2.2.2. Nitrate determination. Following soil identification, three techniques were investigated for nitrate estimation: band integration, cross-correlation, and principal component analysis (PCA) followed by a neural network.

1. **Band integration.** In this simple method, the area below the nitrate absorbance band was used as a predictor, as outlined in Fig. 1. Since the absorbance band associated with nitrate is rather broad and overlaps

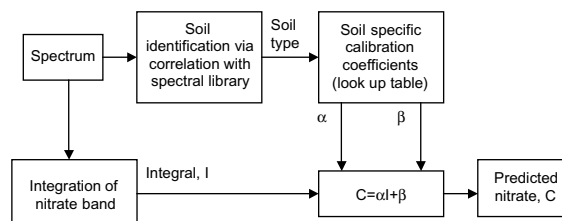


Fig. 1. Schematic representation of the band integration procedure for nitrate determination. C—predicted nitrate concentration, I—area of the $1300\text{--}1350 \text{ cm}^{-1}$ band.

other bands, the “nitrate band” interval over which the integration was performed was not defined a priori, but rather a search was conducted to determine the spectral interval that led to the best results. The search was conducted in the 1200–1500 cm^{-1} range, which includes the ν_3 band and a portion of the interfering carbonate band. The best results were obtained using the 1300–1350 cm^{-1} region, and only these results are reported here.

2. Cross-correlation. Cross-correlation, which is also called matched filtering, is typically used to detect a known waveform in random noise (e.g. Smith, 1997), and is a measure of the similarity between an unknown signal and a reference one. In the present case, since the location of the nitrate absorbance band was known (and fixed), the cross-correlation was reduced to the scalar product between the measured spectrum and the reference one. Conceptually, this approach is similar to the one shown in Fig. 1, with the integration element replaced by cross-correlation. The spectral interval used was the same as for the integration, namely 1300–1350 cm^{-1} .

3. PCA/neural network. The third method consisted of a combination of principal component analysis (PCA) (e.g., Jolliffe, 1986) and a sigmoid-feedforward neural network (e.g., Haykin, 1999). Neural networks (NN) have become popular as “black-box” models that can map any non-linear relationship between input and output variables. With respect to spectroscopy, NN have been used in conjunction with PCA, and in such cases, the PCA scores were used as inputs of the NN (e.g. Ruckebusch et al., 2001; Fidencio et al., 2002). In the present case, the neural network had for inputs not only the PCA scores, but also the soil type, as shown in Fig. 2. In this manner, the NN was able to create a relationship between the PCA scores and nitrate concentration that was soil-dependent. The PCA decomposition range was chosen after a search within the 1300–1500 cm^{-1} range, and only the best results, which were obtained using the narrower 1300–1400 cm^{-1} interval, are presented below.

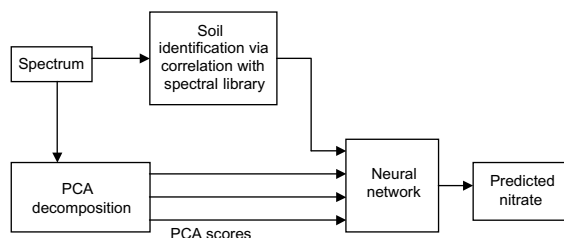


Fig. 2. Schematic representation of the principal component analysis (PCA)/neural network procedure for nitrate determination.

In the following, all nitrate prediction errors are presented in terms of the root mean square error (RMSE):

$$\text{RMSE} = \sqrt{\frac{\sum_{i=1}^N (y - y')^2}{N}} \quad (2)$$

where y and y' are the predicted and actual concentrations, and N is the number of spectra.

3. Results

3.1. Typical spectra and water subtraction

Fig. 3 shows typical spectra of de-ionized water, de-ionized water with 1000 $\text{mg[N]}/\text{kg[water]}$ nitrate, and H2 soil paste with 870 $\text{mg[N]}/\text{kg[water]}$ of added nitrate. The two absorbance bands characteristic of water (e.g. Libnau et al., 1994) are clearly visible in all the spectra. The first band (ν_2) centered around 1640 cm^{-1} is much larger than the nitrate bending band (ν_3) visible in the spectra of the samples with 1000 $\text{mg[N]}/\text{kg[water]}$ and 870 $\text{mg[N]}/\text{kg[water]}$ nitrate (thin and dashed lines). In the spectrum of the water sample with nitrate, a weaker nitrate band (ν_1) is also visible around 1040 cm^{-1} , but due to other soil constituents this band is not visible in the soil spectrum. Careful examination of Fig. 3 shows that, as mentioned in the previous section, the spectra are slightly scaled, biased or tilted relative to each other, and the magnitude of the changes is comparable with the size of the nitrate band. This can be observed, for instance, in the circled regions in Fig. 3.

Fig. 4 shows spectra obtained after applying the water subtraction procedure described above. As

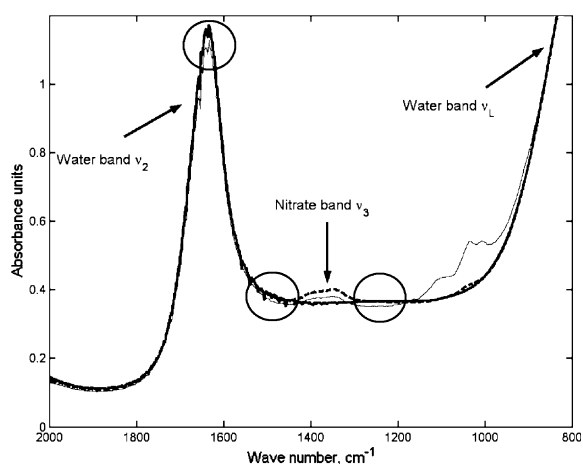


Fig. 3. Spectra of de-ionized water (bold), de-ionized water with 1000 $\text{mg[N]}/\text{kg[water]}$ nitrate (dashed) and H2 soil paste with 870 $\text{mg[N]}/\text{kg[water]}$ nitrate (thin). Regions where the effects of scaling and baseline changes are clearly visible are circled.

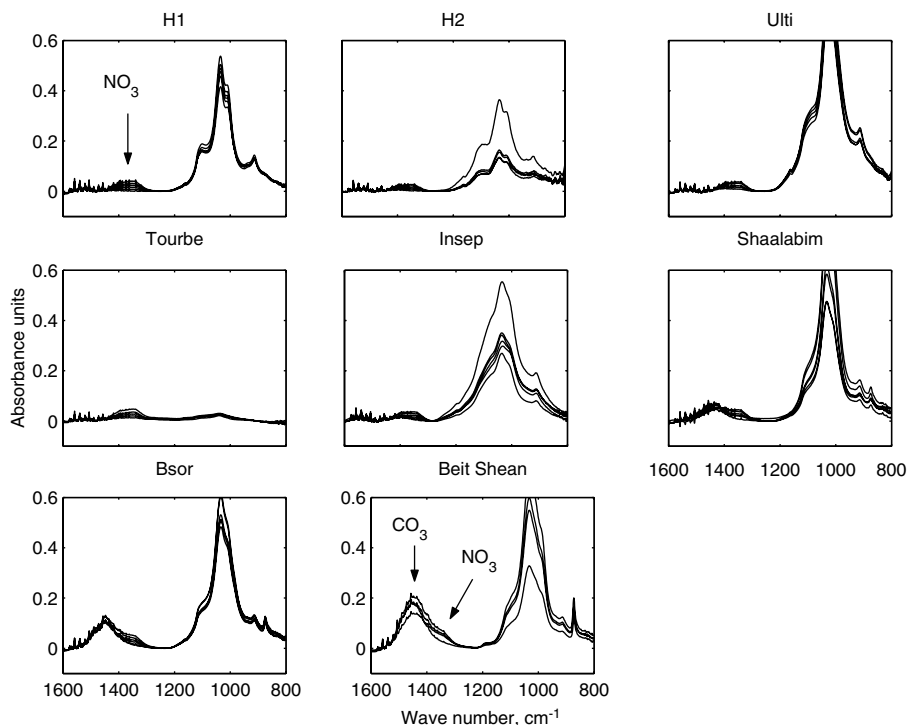


Fig. 4. Typical spectra of soil pastes after water subtraction and baseline correction. In each frame, the different lines correspond to various nitrate concentrations in the soil paste.

expected, the ν_3 nitrate band and the “fingerprint region” ($800\text{--}1200\text{ cm}^{-1}$) have been enhanced, while the water contribution has been cancelled. The “noise” in the $1440\text{--}1580\text{ cm}^{-1}$ interval is due to water vapor in the optic path (e.g. Stuart, 1997).

3.2. Soil identification and nitrate determination

Fig. 4 shows spectra obtained for seven different soils and the peat pastes after proper subtraction of the water spectrum and baseline correction. In the three calcareous soils (Shaalabim, Bsor and Beit Shean), a clear band around 1450 cm^{-1} is observed, which is associated with the ν_3 carbonate bending and increases with total carbonate content. In the non-calcareous soils, the much smaller nitrate absorbance band can be seen in the $1300\text{--}1400\text{ cm}^{-1}$ region. For the Shaalabim, Bsor and Beit Shean soils, this band is distorted and barely visible. Each soil appears to have a distinctive “fingerprint” in the $800\text{--}1200\text{ cm}^{-1}$ region, most probably due to its mineral and possibly organic constituents. Nitrate concentration affects the amplitude of the “fingerprint”, but not its shape (i.e. the ratio between bands), so that the correlation method described above for identifying the soils, which is insensitive to the amplitudes of the spectra, is appropriate.

As expected from Beer–Lambert law, a strong linear correlation exists between the nitrate concentration and the integral of the nitrate absorbance band (calculated over the $1300\text{--}1350\text{ cm}^{-1}$ interval). However, as shown

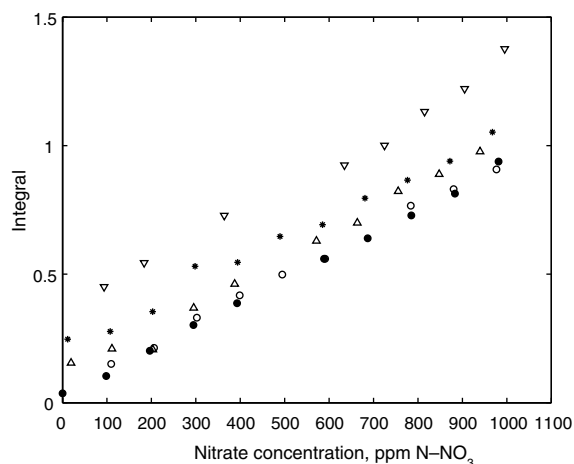


Fig. 5. Integral of the nitrate absorbance band ($1300\text{--}1350\text{ cm}^{-1}$ interval) vs. nitrate concentration of the soil pastes. (●) H1, (○) Ulti, (△) Shaalabim, (*) Bsor, (▽) Beit Shean. Other non-calcareous soils not shown for clarity.

Table 2
Nitrate determination errors

Soil	Prediction error (mg[N]/kg[dry soil])		
	Integration of the 1300–1350 cm^{-1} interval	Cross-correlation over the 1300–1350 cm^{-1} interval	PCA and NN applied to the 1300–1400 cm^{-1} interval
H1	5.46	5.85	4.29
H2	5.50	5.00	3.60
Ulti	6.75	6.30	4.05
Tourbe	134.84 (89.00)	134.84 (89.00)	81.88 (81.88)
Insep	12.60	11.40	6.60
Shaalabim	23.87	24.64	20.02
Bsor	12.80	12.80	8.80
Beit Shean	16.92	17.39	6.58

Results based on identified soil, except numbers in parenthesis for Tourbe, which were obtained using the correct soil.

in Fig. 5, this correlation strongly depends on the type of soil. All three calcareous soils (Shaalabim, Bsor and Beit Shean) have large (but different) non-zero intercept due to the interference of the 1450 cm^{-1} band (Fig. 4).

The results relative to nitrate determination are summarized in Table 2. These results are presented on a dry soil basis (which is of practical interest) despite the fact that nitrate is highly soluble in water and is present only of the liquid phase of the paste. (e.g. Page et al., 1982). The necessary unit conversion is based on the paste moisture values listed in Table 1.

Combining soil identification with calibration curves such as those shown in Fig. 5 (according to the scheme shown in Fig. 1) leads to the nitrate concentration prediction errors summarized in the second column of Table 2. Clearly, misidentification of the soil could cause large errors. However, misidentification occurs only once (Tourbe, identified as Insep). For that case, the error obtained using the correct calibration curve (equivalent to correct soil identification, or soil type known a priori) is given in parenthesis in Table 2. Tourbe excluded, the errors range from approximately 6 to $24 \text{ mg[N]/kg[dry soil]}$, depending on soil composition. The large error for Tourbe is somewhat misleading, as it is due to the very high moisture content of the saturated paste of the peat (356%). In terms of nitrate concentration in the solution, mg[N]/g[water] , the error for Tourbe is similar to the errors obtained for all the other soils ($\approx 10\text{--}40 \text{ mg[N]/kg[water]}$). The largest prediction errors for the mineral soils were obtained for the calcareous ones (Shaalabim, Bsor and Beit Shean), which agrees with the previous observation that the carbonate band interferes with the nitrate band, and shows that soil identification reduces the effect of the interference but does not eliminate it completely.

The results from the cross-correlation approach (third column in Table 2) are almost identical to those obtained by simple integration, showing that, in the

present case, there is no advantage of the cross-correlation method over the simpler integration approach.

The results based on PCA decomposition of the $1300\text{--}1400 \text{ cm}^{-1}$ interval followed by a neural network are shown in the last column of Table 2. The number of scores used as input for the neural network, as well as the number of hidden nodes, were varied from two to six, and the results presented in Table 2 were obtained using the first three scores and three hidden nodes. Using additional scores or hidden nodes did not improve the predictions, while using only one or two scores or hidden nodes led to very poor results (not shown). Comparison of the second, third and fourth column of Table 2 shows that the PCA/neural network approach leads to smaller prediction errors than the integration and cross-correlation methods. The most significant improvement was obtained with soils containing CaCO_3 , and in particular Beit Shean, for which the prediction error was reduced by more than 50%.

For practical applications, light soils, such as H1 and H2, are of special interest since on the one hand they are suitable for intensive agriculture, and on the other hand they are the most sensitive both in terms of nitrate pollution and agronomic response to nitrogen application management. For such soils, the prediction errors are around $4 \text{ mg[N]/kg[dry soil]}$ or less.

4. Conclusions

Attenuated total reflection spectroscopy in the mid-IR range appears to be a promising tool for direct and close to real-time determination of nitrate concentration in soils, with minimal treatment of the samples. After accurate subtraction of the water spectrum, a strong correlation between the nitrate concentration and the ν_3 nitrate bending band can be found. This correlation is soil-dependent, due mostly to varying carbonate

contents and possibly other soil constituents that interfere with this nitrate absorbance band. Accordingly, a two-stage method has been developed, in which the type of soil is identified first, so that the appropriate calibration curve can be used. Combining soil identification with PCA decomposition and a neural network further improved the predictions of nitrate concentration, especially with soils containing CaCO₃. Typical prediction errors are as low as 4 mg[N]/kg[dry soil] or less for non-calcareous light soils. Such soils are of special interest since they are suitable for intensive agriculture, their yield is very sensitive to N-application management, and they are most vulnerable in terms of nitrate pollution. For soils containing calcium carbonate, the errors range from approximately 6 to 20 mg[N]/kg[dry soil].

These errors are appreciably lower than the ones reported in a previous paper based on the same soils (Linker et al., 2004), in which similar chemometric methods (partial least square and cross-correlation) were used in a more conventional manner, i.e. calibrating a single regression model for all the soils. Such an improvement may seem trivial since there are now in fact eight models rather than one. However, it must be remembered that, at the validation stage, model selection is done automatically, based on the “fingerprint” region of the spectrum, and incorrect identification of the soil could result in very poor predictions. While the simple correlation method used here may be expected to perform more poorly when used with a much wider variety of soils, it should be viewed only as a first step toward a more complex “soil identification” tool based on mid-IR spectra. Work in this direction is currently under way in our Department, and includes, for instance, using neural network classifiers or information from other regions of the spectra. Such a tool would help reducing the inherent interferences due to soil constituents when using FTIR/ATR spectroscopy for direct determination not only of nitrate, but possibly also of other soil nutrients or polluting compounds.

Acknowledgement

This study has been supported by the Grand Water Research Institute (GWRI) at the Technion-ITT, and by the US-Israel Binational Research and Development Fund (BARD Project US-3293-20c). Dr. Linker acknowledges the financial support of the Zeff Fellowship.

References

Adsett, J.F., Thottan, J.A., Sibley, K.J., 1999. Development of an automated on-the-go soil nitrate monitoring system. *Appl. Eng. Agric.* 15, 351–356.

- Birrell, S.J., Hummel, J.W., 2000. Membrane selection and ISFET configuration evaluation for soil nitrate sensing. *Trans. ASAE* 43, 197–206.
- Dousseau, F., Therien, M., Pezolet, M., 1989. On the spectral subtraction of water from the FT-IR spectra of aqueous solutions of proteins. *Appl. Spectrosc.* 43, 538–542.
- Ehsani, M.R., Upadhyaya, S.K., Fawcett, W.R., Protsailo, L.V., Slaughter, D., 2001. Feasibility of detecting soil nitrate content using a mid-infrared technique. *Trans. ASAE* 44 (6), 1931–1940.
- Elzinga, E.J., Peak, D., Sparks, D.L., 2001. Spectroscopic studies of Pb(II)-sulfate interactions at the goethite-water interface. *Geochim. Cosmochim. Acta* 65, 2219–2230.
- Fidencio, P.H., Poppi, R.J., de Andrade, J.C., 2002. Determination of organic matter in soils using radial basis function networks and near infrared spectroscopy. *Anal. Chim. Acta* 4583, 125–134.
- Haykin, S., 1999. *Neural Networks. A Comprehensive Foundation*. McMillan College Publishing, New York, USA.
- Johnston, C.T., Aochi, Y.O., 1996. Fourier transform infrared and Raman spectroscopy. In: Bartels, J.M., Bigham, J.M. (Eds.), *Methods of Soil Analysis, Part 3*. Soil Science Society of America Inc., Madison, USA.
- Jolliffe, I.T., 1986. *Principal Component Analysis*. Springer-Verlag, New York, USA.
- Libnau, F.O., Kvalheim, O.M., Christy, A.A., Toft, J., 1994. Spectra of water in the near- and mid-infrared region. *Vibrat. Spectrosc.* 7, 243–254.
- Linker, R., Kenny, A., Shaviv, A., Singher, L., Shmulevich, I., 2004. FTIR/ATR nitrate determination of soil pastes using PCR, PLS and cross-correlation. *Appl. Spectrosc.* 58 (5), 516–520.
- Messica, A., Greenstein, A., Katzir, A., 1996. Theory of fiber-optic, evanescent-wave spectroscopy and sensors. *Appl. Opt.* 35, 2274–2284.
- Page, A.L., Miller, R.H., Keeney D.R., 1982. *Methods of Soil Analysis—Part 2*, second ed. Madison, Wisconsin.
- Powell, J.R., Wasacz, F.F., Jakobsen, R.J., 1986. An algorithm for the reproducible spectral subtraction of water from the FT-IR spectra of proteins in dilute solutions and absorbed monolayers. *Appl. Spectrosc.* 40, 339–344.
- Rahmelow, K., Hübner, W., 1997. Infrared spectroscopy in aqueous solution: Difficulties and accuracy of water subtraction. *Appl. Opt.* 51, 160–170.
- Ruckebusch, C., Sombret, B., Froidevaux, R., Huvenne, J.-P., 2001. On-line mid-infrared spectroscopy data and chemometrics for the monitoring of an enzymatic hydrolysis. *Appl. Spectrosc.* 55, 1610–1617.
- Shaviv, A., Kenny, A., Shmulevich, I., Singher, L., Reichlin, Y., Katzir, A., 2003. IR fiberoptic systems for in situ and real time monitoring of nitrate in water and environmental systems. *Environ. Sci. Technol.* 37, 2807–2812.
- Smith, S.W., 1997. *The Scientist and Engineer's Guide to Digital Signal Processing*. California Technical Publishing, San Diego, USA.
- Stuart, B., 1997. Biological applications of infrared spectroscopy. In: Ando, D.J. (Ed.), *Analytical Chemistry by Open Learning*. John Wiley & Sons, Chichester, USA.